Nuclear Instruments and Methods in Physics Research A 628 (2011) 376–380

Contents lists available at ScienceDirect

Nuclear Instruments and Methods in Physics Research A

journal homepage: www.elsevier.com/locate/nima

Performance of the liquid xenon detector for the MEG experiment

Yasuhiro Nishimura *, Hiroaki Natori

The University of Tokyo, 7-3-1 Hongo, Bunkyo-ku, Tokyo 113-0033, Japan

On behalf of the MEG collaboration

ARTICLE INFO

Available online 6 July 2010

Keywords:
Liquid xenon scintillator
Lepton flavor violation

ABSTRACT

A 900-l liquid xenon (LXe) detector was constructed for the MEG experiment to look for $\mu^+ \to e^+\gamma$. With proper calibration and monitoring the detector was successfully operated during the first physics data taking for three months in 2008. We evaluated the performance of the LXe detector around the signal−γ energy of 52.8 MeV by using 54.9-MeV photons obtained from π^0 decays.

1. Introduction

In 2008 the MEG experiment started physics data taking at Paul Scherrer Institut (PSI) in Switzerland. Our goal is to search for the $\mu^+ \to e^+\gamma$ decay with a sensitivity of 10^{-13} branching ratio, which is by two orders of magnitude better than the present experimental upper bound [1], while well-motivated models of new physics such as SUSY-GUT predict sizable branching ratios within the reach of our experiment.

2. LXe detector

2.1. Design

The MEG detector consists of a spectrometer with a gradient magnet field, low-mass drift chambers and scintillation timing-counter arrays for the measurement of the positrons, and a LXe detector for the detection of γ rays with 10% of the solid angle.

The construction of the 900-l LXe detector equipped with 846 photomultiplier tubes (PMTs) on six faces was completed in 2007 (Fig. 1). This detector measures the energy, timing and position of γ rays by using the excellent properties of liquid xenon. The fast scintillation light with decay-time components of 4.2, 22 and 45 ns [2] and use of a 1.6 GHz waveform digitizer for all PMTs are essential for the good performance of the timing measurement in a high-rate environment. Also, the high light yield of xenon allows obtaining good energy and timing performance.

2.2. Cryogenics and purification system

The cryogenics and the purification system for the LXe detector [3] are illustrated in Fig. 2. The liquid xenon is stably kept around 165 K in a detector cryostat with a pulse tube refrigerator specially developed for the MEG experiment and occasionally also cooled using liquid-nitrogen cooling pipes. The latter is useful especially for the liquefaction of the xenon. During the maintenance of the detector the liquid xenon can be transferred to a 1000-l dewar tank in the liquid phase or to eight high-pressure tanks in the gas phase.

Since the vacuum ultra-violet (VUV) scintillation light of xenon can be easily absorbed by contaminations in xenon, two types of purification systems were developed. The first system is a gaseous purification where evaporated gaseous xenon goes through a getter, which removes H_2O, O_2, CO, CO_2, H_2, N_2 and hydrocarbon molecules and is then re-condensed in the detector. The second system is a liquid-phase purification, where the liquid xenon, taken from the lower part of the detector, goes through molecular sieves and copper beads to remove water and O_2 and then returns to the detector.

3. Calibration

The gain and the quantum efficiency of each PMT are frequently calibrated and monitored using LEDs and ^{241}Am α−sources installed in the liquid xenon. In order to monitor the light yield of xenon, radiative muon decays ($\mu^+ \to e^+ \nu_e \overline{\nu_\mu} \gamma$), cosmic muons and the γ rays from nuclear reactions induced by protons from a Cockcroft–Walton (CW) accelerator are used.

Monochromatic γ rays with several energies are available by using different target nuclei for the CW accelerator. The energy spectra measured in the LXe detector are shown in Fig. 3. The 17.6-MeV γ line from ^{7}Li(p,γ)^{8}Be is especially useful to investigate the non-uniformity of the detector response as well as to monitor the light yield. Cascade γ rays of 4.4 and 11.7 MeV from ^{11}B(p,γ)^{12}C allow to calibrate the relative timing between the LXe detector and the timing counter arrays for the positron measurement. The calibration using the CW accelerator was frequently performed during the physics data taking period to

* Corresponding author.
E-mail address: nisimura@icepp.s.u-tokyo.ac.jp (Y. Nishimura).

0168-9002/$ - see front matter © 2010 Elsevier B.V. All rights reserved.
doi:10.1016/j.nima.2010.07.005

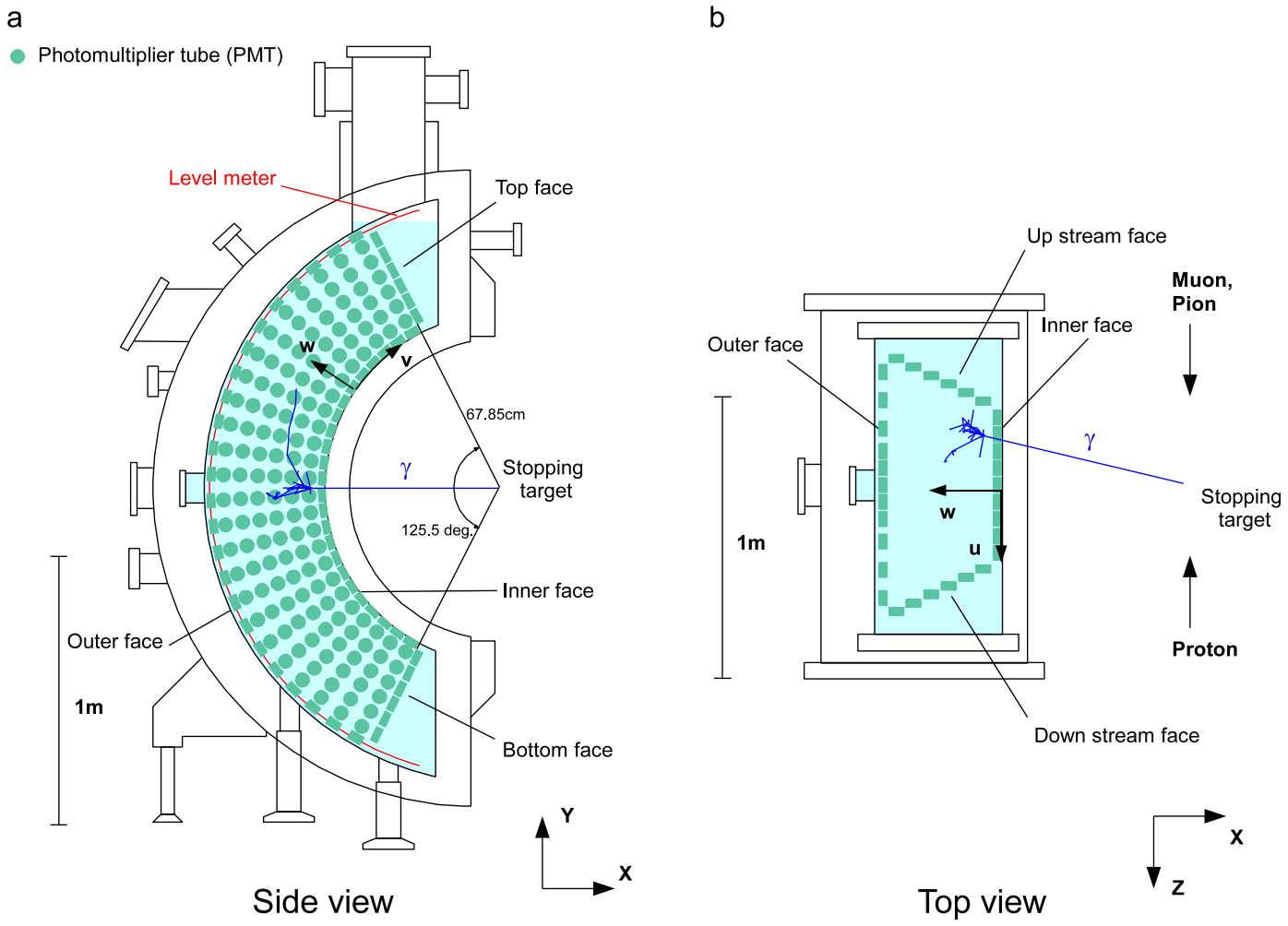

Fig. 1. Schematic view of the LXe detector.

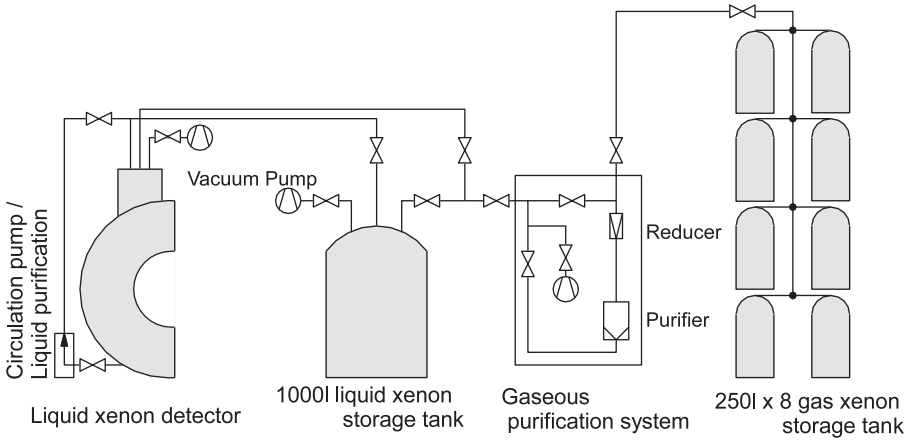

Fig. 2. Cryogenics and purification system of the LXe detector.

monitor the status of the LXe detector because the CW beam line is placed at the opposite side of the muon beam line and we can quickly switch beam modes.

Pion decay ($\pi^0 \rightarrow \gamma\gamma$) following the charge-exchange (CEX) reaction ($\pi^- p \rightarrow \pi^0 n$) induced by π^- stopped in a hydrogen target is quite useful for the performance evaluation of the detector because almost monochromatic γ rays of 54.9 MeV, which is close to the signal γ energy, are obtained by selecting back-to-back events in $\pi^0 \rightarrow \gamma\gamma$.

4. Run 2008

In 2008 we had two π^0−decay runs, one for a month in August before starting the physics data taking and another for a week in December after the physics data taking for three months.

The scintillation light yield in 2008 was monitored by using the 54.9-MeV peak from π^0 decays, the 17.6-MeV peak produced by CW and cosmic-ray peaks as shown in Fig. 4. The light yield was increased by about 40% during the physics data taking

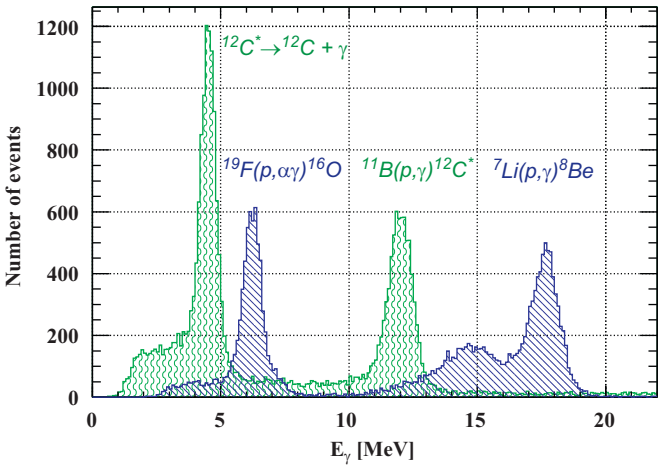

Fig. 3. Energy spectra measured in LXe detector for γ rays from nuclear reactions induced by protons from CW accelerator.

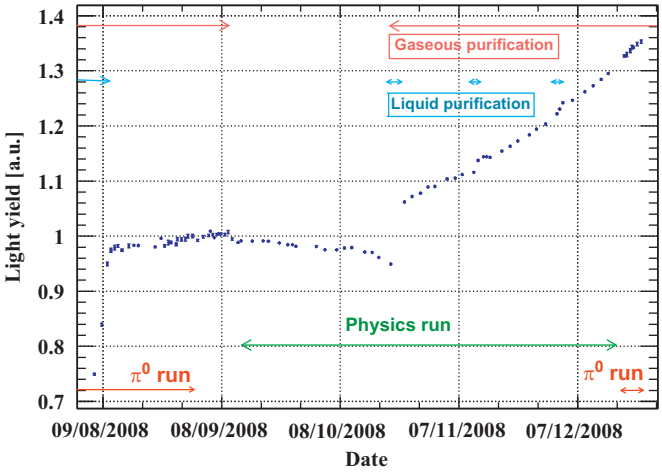

Fig. 4. The light-yield history in 2008.

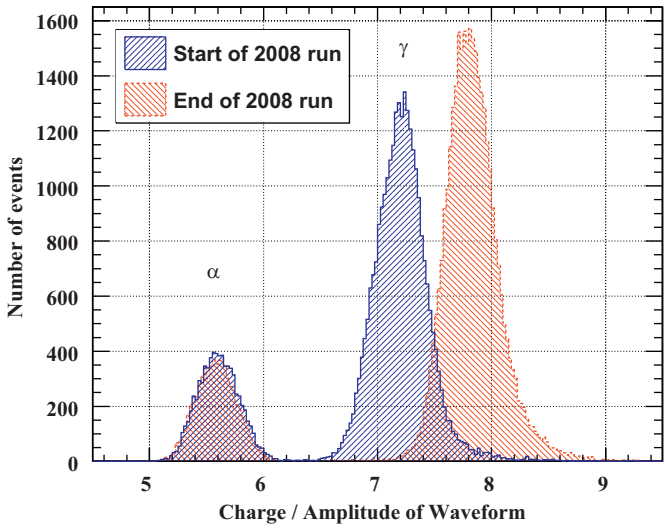

Fig. 5. Discrimination between α−ray and γ−ray.

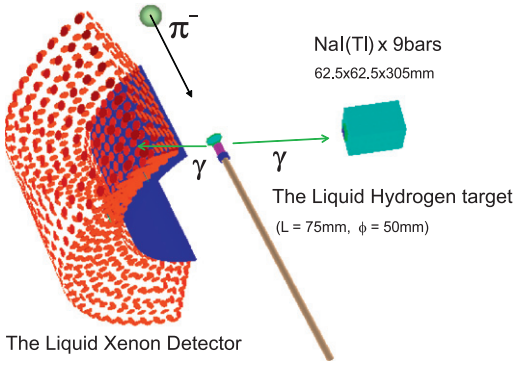

Fig. 6. Setup for the π^0−decay measurement.

especially since the end of October when the purification restarted with full performance. The change of the light yield was monitored with a precision of 0.18% and then the energy scale of the detector determined in the August π^0 run was adopted for all 2008 runs after taking into account the change of the light yield.

The purification of the liquid xenon caused a change in the shape of the waveform for γ rays while the waveform for the α−particles was unchanged. We believe that the purification removed a contamination which suppresses the scintillation process and is only relevant for the γ−ray interaction. Fig. 5 shows that the distribution of the charge-amplitude ratio, which is measured in a waveform summed over all the PMTs, can clearly separate γ from α. Due to the changed γ−ray waveform the separation became better after the purification.

5. Performance

5.1. Setup

The performance of the LXe detector around the signal energy is measured using almost monochromatic γ rays of 54.9 or 82.9 MeV obtained from back-to-back π^0 decays in CEX reactions. One of the two γ rays is tagged by a set of nine NaI(Tl) crystals, which is movable to calibrate the whole acceptance of the LXe detector (Fig. 6).

Scintillation photons from the NaI(Tl) crystals are collected by avalanche photodiodes (APDs) since the detector is placed in the stray magnetic field of the spectrometer magnet. The temperature of the APD is controlled by a cooling system based on a Peltier device to stabilize the gain.

5.2. Energy

The γ energy is reconstructed by summing the number of photons observed by all the PMTs with constant weights and then correcting by the solid angle and the non-uniformity effect.

The energy spectrum shown in Fig. 7 is obtained for the 54.9-MeV γ by selecting the event where the 82.9-MeV γ is detected at the NaI with an opening angle larger than 175° and the reconstructed position in the LXe detector is deeper than 2 cm from the inner face. For the estimation of the energy resolution, the peak is fitted with a combined function of a Gaussian upper part and an exponential lower tail convoluted with the pedestal distribution measured in the π^0 run to remove the effect of high-rate background from the π^- beam. The lower tail in this figure comes from the energy loss due to conversion before reaching the xenon and also from the energy leakage near the face of the detector. The energy resolution of the upper part is more important to distinguish signal γ from background.

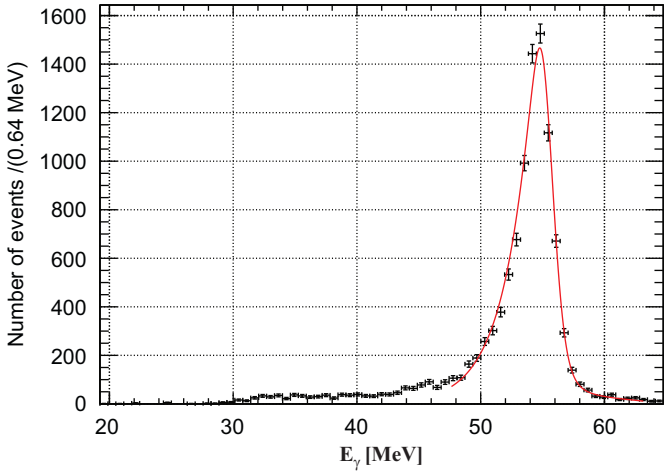

Fig. 7. Measured energy spectrum of 54.9-MeV γ−rays.

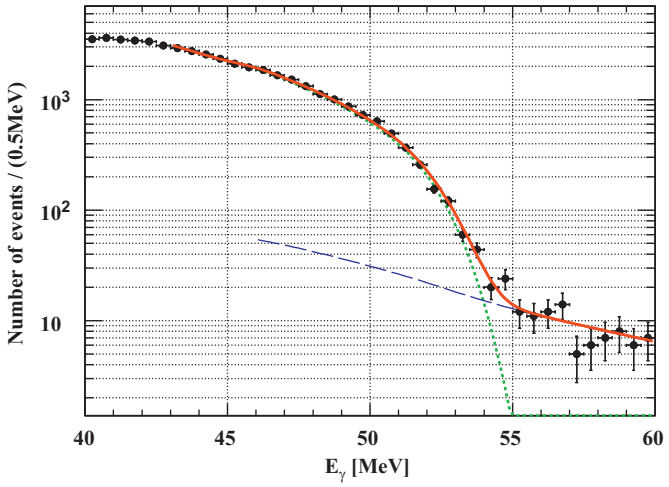

Fig. 8. Measured background spectrum of γ−rays during physics data taking. The solid line shows the MC spectrum smeared by the resolution.

An average energy resolution of $\Delta E/E = (5.8 \pm 0.35)\%$ FWHM with a right tail of $\sigma_R = (2.0 \pm 0.15)\%$ around 54.9 MeV is obtained in this measurement.

Fig. 8 shows the energy spectrum of the γ−ray background measured in the physics run. It is consistent with the Monte Carlo spectrum smeared by the resolution measured in the π^0 run.

The systematic uncertainty of the energy scale determined at 54.9 MeV in the π^0 run is estimated to be 0.4% by considering uncertainties of PMT gain drift and the light-yield monitor, the error of fitting for the energy determination and a small difference from the energy scale measured in the physics run.

5.3. Timing

At first the photon arrival time of each PMT is calculated by subtracting the propagation time of photons in xenon and the offset time due to cables and electronics. The time of the γ−interaction is then reconstructed by averaging the time of the PMTs near the incoming position with a weight from the number of photoelectrons.

A lead converter and two plastic counters with four PMTs were placed in front of the NaI in order to detect one of the two coincident γ−rays in the π^0 run, then the timing resolution is estimated by measuring another γ in the LXe detector. In August, the spread of the time difference between the LXe detector and the plastic counters in front of the NaI was 135 ps in σ. The time resolution of the LXe detector is estimated to be 78 ps in σ at 54.9 MeV after subtracting the resolution of the plastic counters (93 ps) and the contribution from the beam spread in the hydrogen target (58 ps). We obtained a better resolution of 68 ps in σ in December because of the improvement in the light yield.

5.4. Position

The γ−ray interaction point is reconstructed by comparing the distribution of the light observed by the PMTs and the distribution of the solid angles subtended by the PMTs to the reconstructed position.

The performance of the position reconstruction is evaluated by Monte Carlo simulation. The resolutions are estimated to be 6 and 5 mm along the radial direction and the inner face of the LXe detector, respectively. A small discrepancy between the Monte Carlo simulation and the measurement in the subsequent dedicated π^0 run is taken into account in the resolution along the inner face.

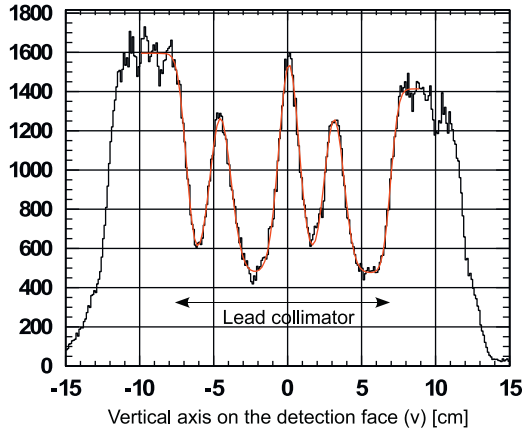

Fig. 9. Reconstructed vertical position on the inner face with a lead collimator for the γ−rays from π^0 decays. The position resolution is estimated from the spread of the three peaks due to the slits after subtracting the effects of the slit width and the target size.

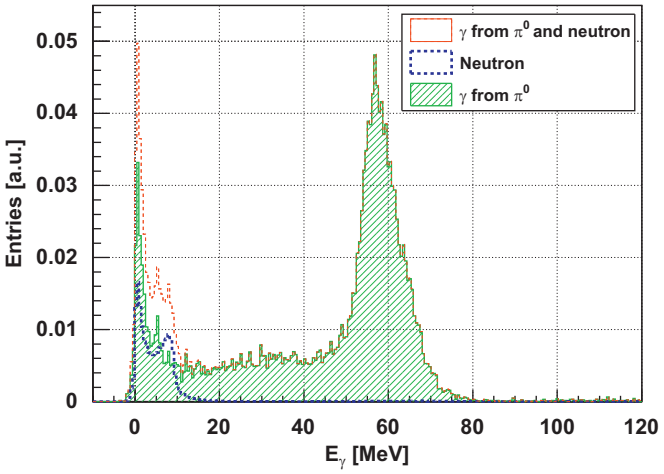

Fig. 10. Energy spectrum in the LXe detector obtained by tagging the more energetic 82.9-MeV γ−ray from $\pi^0 \rightarrow 2\gamma$ at the opposite NaI detector.

In the π^0 run we evaluated the position resolution by placing lead collimators of 1.8 cm thickness and 1-cm slits in front of the liquid-xenon detector. Fig. 9 shows the distribution of the reconstructed position along the vertical direction with the collimator placed at the center of the face. By looking at the reconstructed shadow of the 1-cm slits of the lead, the σ resolution along the inner face was estimated to be 5 mm after subtracting the effect of the width of the slits and the spread of the beam in the target.

5.5. Detection efficiency

Since there is a lower energy tail in the E_γ spectrum, we need to set a threshold to define the detection efficiency. The detection efficiency defined for $E_\gamma > 46$ MeV is estimated to be 67% by using a Monte Carlo simulation.

The detection efficiency was also measured in the π^0 run by calculating the probability to detect 54.9-MeV γ−rays with the LXe detector for the events where the 82.9-MeV γ was detected in the NaI detector. Fig. 10 shows the energy spectrum in the LXe detector obtained by tagging the γ in the NaI detector around 82.9 MeV. The right-hand side of the spectrum is broadened since no opening angle cut is applied. The small peak at low energy is due to neutron background where a monochromatic γ−ray of 129 MeV from the radiative capture ($\pi^- p \to n\gamma$) is detected at the NaI detector by depositing part of the energy while the neutron is detected in the LXe detector. After subtracting the effect of the neutron background we can estimate the detection efficiency to be 62%. The discrepancy between the Monte Carlo simulation and the measurement is 4% after correcting for the threshold effect and is regarded as the uncertainty of the detection efficiency.

Finally we obtained a detection efficiency of (63 ± 4)% in the range of $E_\gamma > 46$ MeV after including the inefficiency of the analysis such as cuts on cosmic rays and pile-up events.

6. Summary

The MEG physics run started on September 12, 2008 and took data successfully for three months with good performance and stability of the LXe detector. We evaluated the energy resolution to be $\sigma_R = (2.0 \pm 0.15)\%$ and the time resolution to be 78 ps in σ at 54.9 MeV near the signal energy in the π^0−decay run, and obtained a position resolution σ of 5 mm along the inner face. The detection efficiency at the signal energy was estimated to be (63 ± 4)%.

References

[1] M.L. Brooks, et al., MEGA Collaboration, Phys. Rev. Lett. 83 (1999) 1521.
[2] T. Doke, Portugal Phys. 12 (1981) 9.
[3] T. Haruyama, et al., Cryogenics 49 (2009) 254.